Journal of

Fall 1990

ENGINEERING TECHNOLOGY

A Publication of the Engineering Technology Division · American Society for Engineering Education

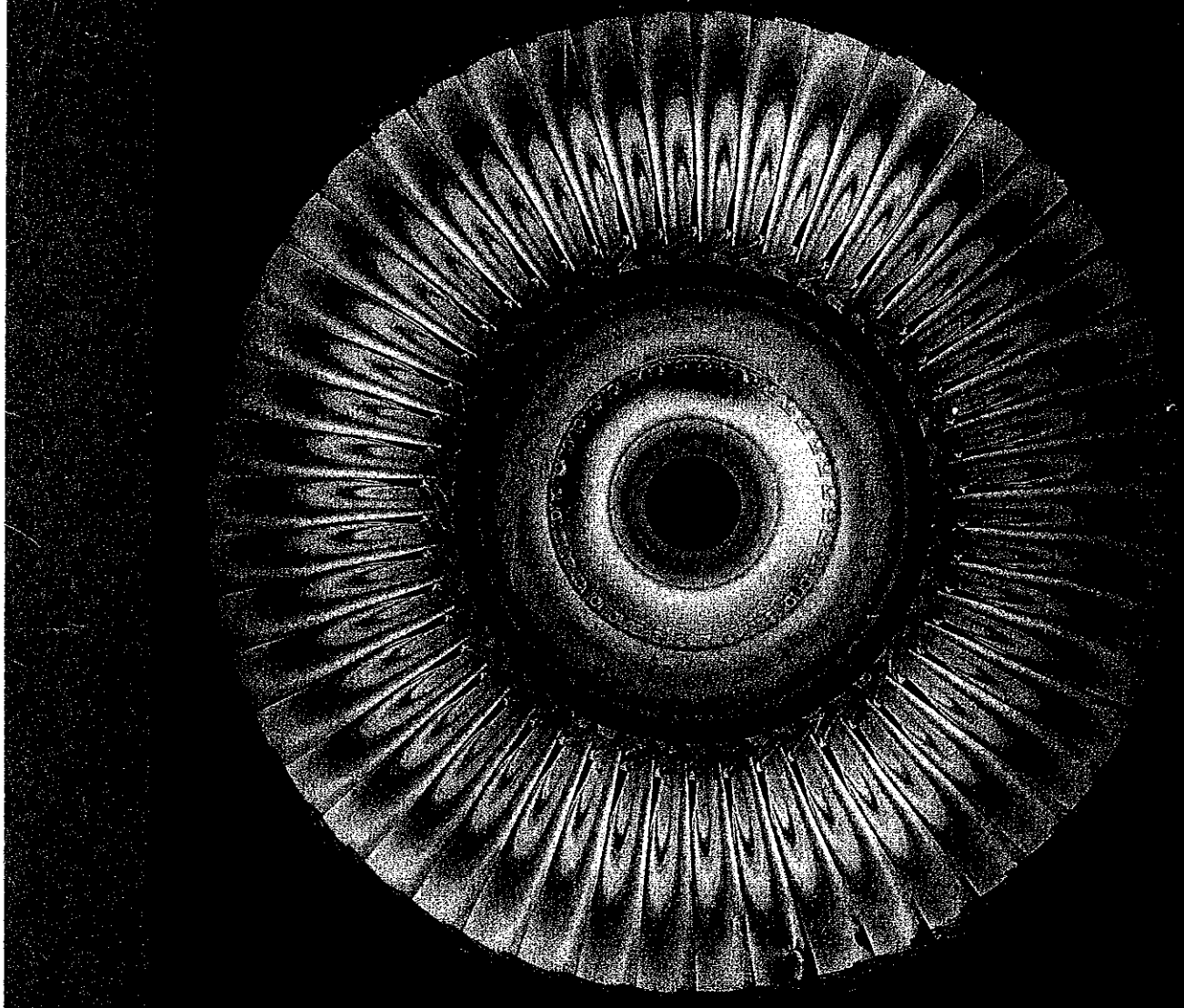

DC Motor-Generator Set...Hybrid Power Plant-Engine...
EET Software...Teaching Plastics Technology...
Oscilloscope Instruction...CAD..."Internal" CO-OP...

Modeling of a Loaded DC Motor-Generator Set in an EET Undergraduate Controls Laboratory

Anthony J. A. Oxtoby, Purdue University
Thomas L. Robertson, Purdue University
J. Michael Jacob, Purdue University

ABSTRACT

The process of obtaining a linear model for a loaded DC motor-generator set which forms part of a closed-loop speed regulation system is described. Further, a comparison of measured and model-predicted dynamic behavior is presented.

INTRODUCTION

In view of the prevalent use of computer simulation and design packages, exposure to the process of formulating a mathematical model to adequately represent the dynamic behavior of the interconnected elements of a system provides a valuable experience for students. Choice of both the hardware and the model is important. Because a loaded DC motor-generator set which forms part of a closed-loop speed regulator can be intuitively understood, its use provides students with a relatively gentle introduction to linear control theory.

Since this material is presented to juniors majoring in electrical engineering technology, a linear model[1] is used rather than more complex non-linear representations.[2] The system, however, exhibits sufficient non-ideal properties and non-linearities to highlight the limitations of the model; students are required to account for these differences.

Model development is performed in the following stages, with each step permitting a comparison between model and measured behavior.

* Model of the unloaded motor driven from a Hampden DC supply
* Model of the DC generator and a resistive load
* Model of the speed sensor

LABORATORY EQUIPMENT

With the exception of the controller, the system hardware is depicted in figures 1 and 2. An Action Pack AP 3231 DC input/Phase-Angle Thyristor Firing Bridge module is shown cascaded with an AP 3010 Thyristor/Diode Bridge module in order to control the 0 to 115 VDC armature voltage of the motor from an analog voltage of 0 to 10 V. Note that a snubber circuit must be included across the thyristor bridge output terminals. This consists of a 0.3 μF, 500 V capacitor in series with a 300 Ω, 1/2 W resistor. The resistor is shunted by a reverse-biased IN4007 diode. The motor shaft speed is measured using an Allen-Bradley type 845N-SJDN3-CMY1 500 pulse/rev optical incremental encoder which is coupled directly to the shaft. A signal varying from 0 to 20 kHz, which corresponds to a motor speed range of 0 to 2400 rpm, is then fed to an Action Pack model 7010-1914S frequency-to-voltage converter to produce an analog signal of 0 to 10 V.

The field windings of the motor and generator are supplied at 115 VDC from a Hampden model HMD-100-PPC DC voltage supply which is also used during transient tests to verify the model of the motor. A 1/3 hp, separately excited Reliance motor (Hampden model DCM-100) is coupled to a Reliance 1/8 kW generator (Hampden model DCG-100) which, in turn, drives a resistive load of up to 120 W.

BLOCK DIAGRAM FORMATION

Control systems are commonly represented in block diagram form. If these systems are depicted in such a manner, the overall system transfer functions can easily be obtained, using block diagram reduction methods, in a form suitable for use with computer simulation packages such as Program CC[3] or those associated with control texts.[4] A second benefit of this approach is that the process of converting schematics to block diagrams causes the student to focus on the fundamental operations of the systems—a valuable exercise.

For example, the block diagram of the unloaded DC motor of figure 3 may be established in simple stages. The relationship between the mechanical variables—applied torque T, the input, and shaft speed ω, the output—may be obtained by applying Newton's law of motion for a fixed moment of inertia. Thus, the net torque needed to accelerate a motor is

$$T - B_m\omega = J_m\frac{d\omega}{dt} \qquad (1)$$

where J_m = polar moment of inertia of the motor armature,
B_m = coefficient of viscous friction.

Taking the Laplace transform of equation (1) and assuming zero initial conditions for ω and T, we obtain

$$\left[T(s) - B_m\omega(s)\right]\frac{1}{J_m} = s\omega(s) \qquad (2)$$

Similarly, for the armature circuit the input voltage, V_i, and the output armature current are related by Kirchhoff's voltage law.

Applying Laplace transforms to the armature circuit and again assuming zero initial conditions, we obtain

$$V_i(s) - k_e\omega(s) = \left(R_a + sL_a\right)I_a(s) \qquad (3)$$

Equations (2) and (3) are implemented at the right and left-hand summing junctions, respectively, of figure 3 along with a block to account for the motor torque constant k_T. k_T relates the armature current I_a to the motor torque T and the constant term T_c, where the last term, which is described later, accounts for the Coulomb torque.

MEASUREMENT OF MOTOR PARAMETERS FOR THE LINEAR MODEL

This section describes methods for the measurement of the model parameters, the values of which should be confirmed by comparison to manufacturers' data whenever possible.

Determination of the Armature Inertia J_m

The method described here is based upon the measurement

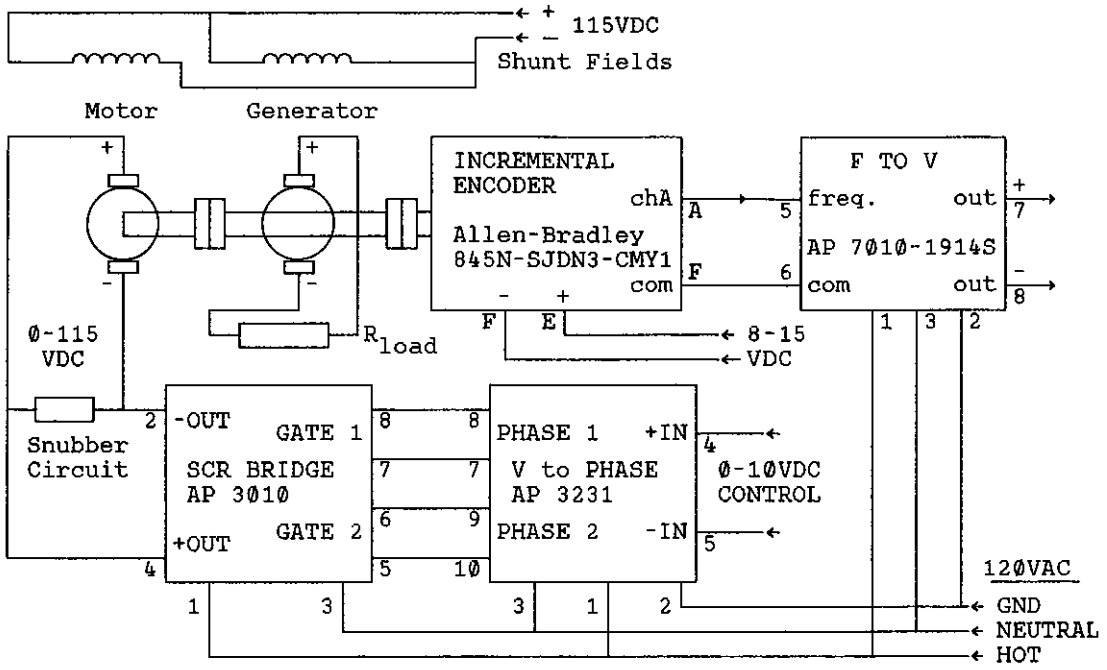

Figure 1. DC Motor Control Electronics

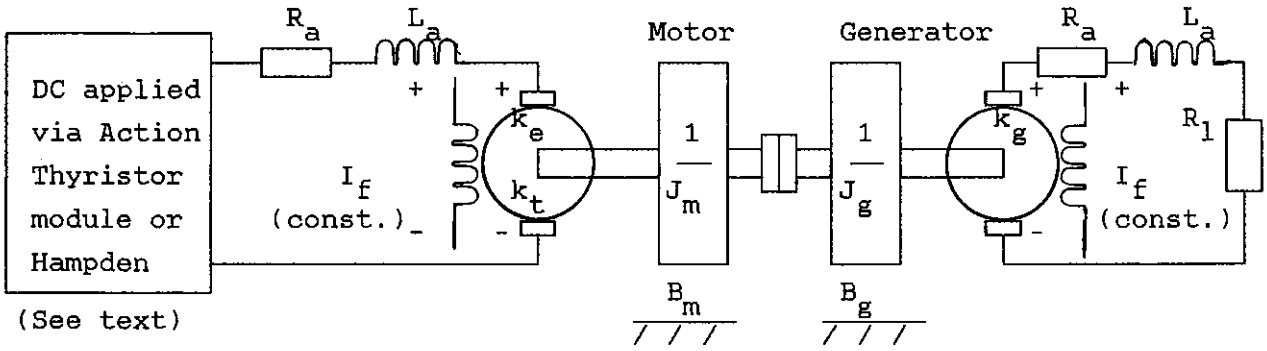

Figure 2. DC Motor-Generator Set Schematic

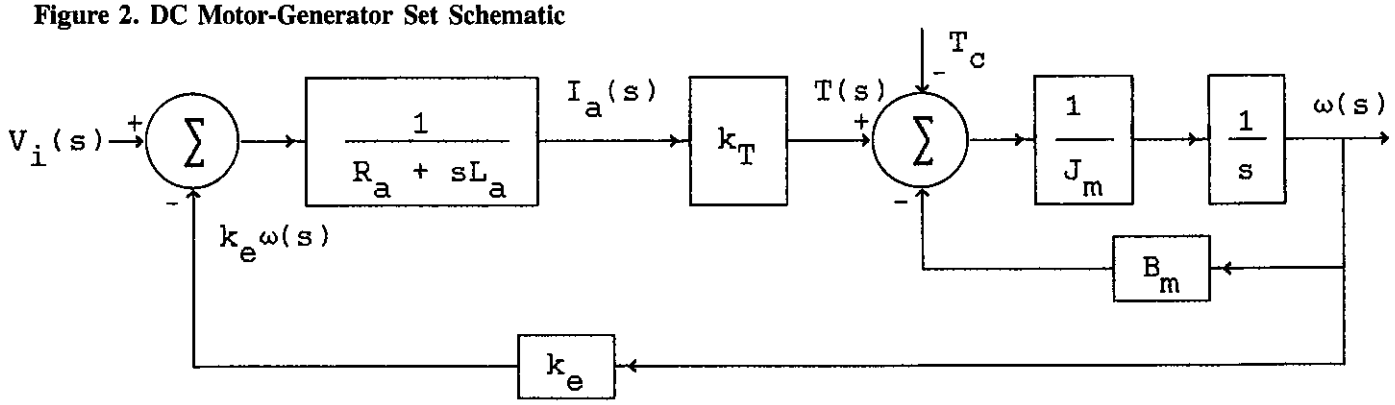

Figure 3. Overall Block Diagram for Unloaded DC Motor

of the period of oscillation of a rotational pendulum. With the armature removed, a length of piano wire (A "top" E guitar string works well!) is attached to the end of the shaft through an eyelet, and the assembly is suspended from a support. The armature is then rotated approximately one-half of a turn and released, and the period of the resulting torsional oscillation is measured; accuracy can be improved by measuring the time required to execute a large number of oscillations. The armature is then replaced by a solid cylindrical mass suspended from the same wire; the period of oscillation is again measured.

The mass moment of inertia, J_r, for a solid cylinder of mass M and radius R is given by

$$J_r = \frac{1}{2} MR^2 \qquad (4)$$

and the period of oscillation of a rotational pendulum is

$$t_r = \frac{1}{2\pi}\sqrt{\frac{J}{k}} \qquad (5)$$

where k is the stiffness of the suspension. The polar moment of inertia of the armature can then be determined from

$$J_m = J_r\left(\frac{t_m}{t_r}\right)^2 \qquad (6)$$

where t_m = period of oscillation for the motor armature (s),
t_r = period of oscillation for the cylindrical mass (s).

Determination of the Back emf Constant k_e

For a fixed value of field voltage (115 VDC), k_e can be obtained by using the motor as a generator and then plotting the open-circuit armature voltage, E_a, as a function of the armature angular velocity ω (rad/s); k_e (V/rad/s) is equal to the slope of the graph.

Determination of the Torque Constant k_T

For a given, fixed value of field excitation (115 VDC in this case), the constant k_T can be obtained from the slope of the graph of motor-developed torque, T, versus armature current, I_a. The torque can be measured by either a dynamometer or a Prony brake.[5] This value of k_T can be checked because if k_T is measured in N·m/A and k_e is measured in V/rad/s (that is, both are in SI units), then k_T and k_e are theoretically numerically equal.[6] Indeed, this method is suggested as an alternative in some texts.[7] Our results have shown a worst case difference of 11% between k_T and k_e.

Determination of the Armature Inductance L_a and the Resistance R_a

The armature inductance depends upon the total flux in the DC machine and, as such, is a non-linear function of both armature and field current. For linear modeling purposes L_a is frequently neglected; however, we felt it was necessary to examine the validity of this assumption by investigating the variation of L_a with I_a for a fixed value of the field current. Measurement of L_a for various values of I_a is based upon determination of the first order growth in armature current when the motor is used as a generator with variable load.[8]

Our measurements showed a similar trend in the variation of L_a with I_a as described by Szabados et. al.[8] Armature inductance decreased approximately 30% to 32 mH during the first 1 A increase in I_a and thereafter declined more slowly to approximately 26 mH as saturation was approached at the rated maximum load current of 3.4 A. We thus considered the value of L_a to be essentially constant over the motor operating range of interest.

Measurement of the armature circuit resistance was performed using Forgue's method.[5] The "cold" value of R_a was 7.5 Ω; this resistance then rose to 8.7 Ω when the motor had been run for 60 minutes under load. In conclusion, a maximum value of inductance of 32 mH with a minimum value of R_a of 7.5 Ω results in a maximum electrical time constant, τ_a, ($\tau_a = L_a/R_a$) of about 4.3 ms.

Determination of Friction Constants

The various forms of frictional losses in machines produce an overall non-linear frictional torque versus speed characteristic, especially at low speeds. These losses are generally represented by a combination of three types of friction: static friction, Coulomb friction, and viscous friction. An attempt has been made to measure two of the three friction coefficients; static friction was neglected because it does not have an effect once motion occurs, and the system is normally not operated from standstill. If only Coulomb and viscous friction are considered, then the expression for the torque of the motor (equation [1]) becomes

$$T = k_T I_a = J_m\frac{d\omega}{dt} + T_c + B_m\omega \qquad (7)$$

where T_c is the Coulomb friction torque.

If the unloaded motor is run at constant speed, then

$$I_a = \frac{T_c}{k_T} + \frac{B_m\omega}{k_T} \qquad (8)$$

Plotting I_a at selected values of ω yields a linear graph whose slope is B_m/k_T and whose y-intercept is T_c/k_T. Results are shown in figure 4. Note that the speed is not decreased below 400 rpm because the deviation from the straight line would become excessive due to non-linear friction effects.

Unloaded DC Motor Model Summary

The following list represents the parameters of the linear model for the Reliance Electric type 437698-TF, separately excited, 1/3 hp DC motor when operating with a field supply of 115 VDC.

$J_m = 18.17 \times 10^{-4}$ kg·m^2
$B_m = 2.4 \times 10^{-4}$ N·m/rad/s
$k_e = 0.48$ V/rad/s
$k_T = 0.45$ N·m/A
$L_a = 32$ mH
$R_a = 7.5\ \Omega$ (cold)
$R_a = 8.7\ \Omega$ (hot)
$T_c = 6.48 \times 10^{-2}$ N·m

MODEL SIMPLIFICATION

Figure 3 is a detailed, linear representation of the dynamic behavior of the unloaded DC motor; because of the model's complexity, it is desirable to simplify it. Any changes must be justified so that students gain an understanding of the effect each of the various parameters has on the model's behavior. Described below are the three parameters which significantly affect the dynamic behavior of the model: L_a, T_c, and B_m.

Armature Inductance L_a

Referring to figure 3, consider the transfer function relating $\omega(s)$ to $V_i(s)$. Using block diagram reduction we obtain

$$\frac{\omega(s)}{V_i(s)} = k_T\Big/\left[s^2L_aJ_m + s\left(L_aB_m + R_aJ_m\right) + \left(R_aB_m + k_ek_T\right)\right] \qquad (9)$$

The roots of the quadratic in the denominator are the open-loop poles of the motor and are in general real and negative. Hence, the roots are

$$s_{1,2} = \frac{-\left(J_mR_a + L_aB_m\right) \pm \sqrt{\left(J_mR_a + L_aB_m\right)^2 - 4J_mL_a\left(B_mR_a + k_ek_T\right)}}{2J_mL_a} \qquad (10)$$

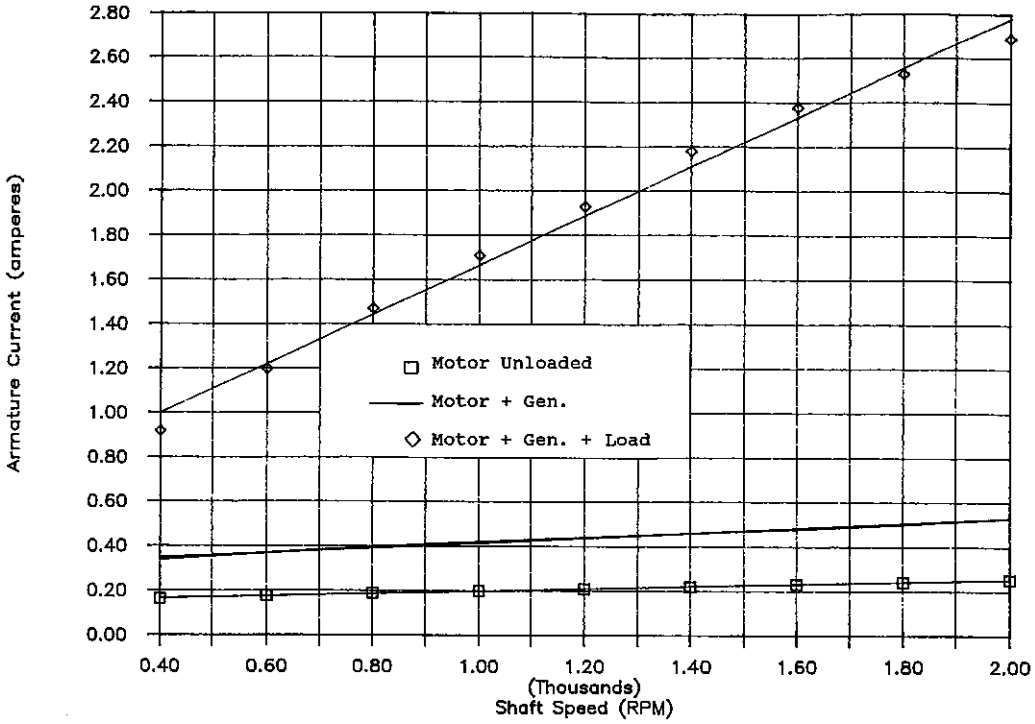

Figure 4. Armature Current vs. Speed for the DC Motor-Generator Set

From the measured data for this motor, we obtain

$$s_1 = -17.1\ s^{-1} \quad \text{and} \quad s_2 = -217\ s^{-1}$$

These two poles correspond to time constants of

$$\tau_1 = -1/s_1 = 58.2\ \text{ms} \quad \text{and} \quad \tau_2 = -1/s_2 = 4.6\ \text{ms}$$

Clearly, pole s_1 is the dominant pole, and s_2, with its correspondingly small time constant, may be neglected; thus, the model may be simplified to one of first order.

Equation (9) can then be factored to obtain

$$\frac{\omega(s)}{V_i(s)} = k_T \Big/ \left[\left(1 + \frac{sL_a}{R_a} \right) \times \left(sJ_mR_a + B_mR_a + \frac{k_ek_T}{1 + \dfrac{sL_a}{R_a}} \right) \right] \quad (11)$$

The electrical time constant, τ_a, is often small; from our model data, $\tau_a = 4.27$ ms, which accounts for the value of τ_2 above. Thus, neglecting τ_a we obtain

$$\frac{\omega(s)}{V_i(s)} = \frac{\dfrac{k_T}{B_mR_a + k_ek_T}}{1 + \dfrac{sJ_mR_a}{B_mR_a + k_ek_T}} \quad (12)$$

where the quantity $J_mR_a/(B_mR_a + k_ek_T)$ is frequently referred to as the mechanical time constant, τ_m.[9] From the model data, $\tau_m = 62.56$ ms (compare this value to that of τ_1 above).

Similar terms are contained in the transfer function relating $\omega(s)$ to $T_c(s)$; thus, terms containing L_a/R_a (the electrical time constant) may again be neglected. The simpler block diagram is shown in figure 5, and it allows the transfer function of equation (12) to be obtained (with T_c equal to zero).

The Effect of Coulomb Friction Torque T_c

This parameter, which is usually not discussed in the literature, has two effects on the behavior of the model. First, it reduces the steady-state value of the armature speed for a given input voltage, as the driving torque is now $T - T_c$.

To examine this effect in more detail, transfer functions $\omega(s)/V_i(s)$ and $\omega(s)/T_c(s)$ are obtained separately from figure 5 and then combined using the superposition principle to obtain

$$\omega(s) = \frac{\dfrac{k_TV_i(s) - T_c(s)R_a}{B_mR_a + k_ek_T}}{1 + \dfrac{sJ_mR_a}{B_mR_a + k_ek_T}} \quad (13)$$

Note that the dynamics are unaffected because the time constant is unchanged. However, the steady-state speed for a value of V_i is reduced by approximately 1% when T_c is neglected.

A second effect of the Coulomb friction torque is that it causes a more rapid deceleration of the motor when power to the armature is removed, at which time the time constant associated with such a test is reduced (by a factor of three in our tests) well below the value $(J_m/B_m)_{predicted}$ when only the viscous friction, B_m, is considered in the braking effect.

For example, in figure 6, in which no armature circuit is involved, the motor has an initial angular velocity $\omega(0)$. The equation of motion—including initial conditions and assuming T_c can be represented by a step function—is

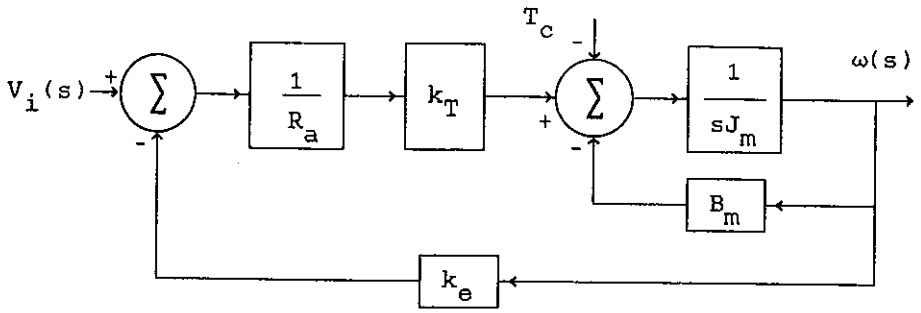

Figure 5. Simplified Block Diagram for Unloaded Motor

$$\frac{-T_c}{s} - B_m\omega(s) = sJ_m\omega(s) - J_m\omega(0) \qquad (14)$$

Hence, in the time domain

$$\omega(t) = \omega(0)e^{-t/\tau} - \frac{T_c}{B_m}\left(1 - e^{-t/\tau}\right) \qquad (15)$$

where τ is the time constant when only viscous friction is considered.

The first term in equation (15) represents the deceleration due to viscous friction, whereas the second term describes the combined effect of viscous and Coulomb friction. Overall, the speed of response is considerably reduced below the value obtained using $\tau = J_m/B_m$. "Run down" tests on the motor, in which the decrease in speed was monitored after open-circuiting the armature, were conducted for several initial speeds. The results are summarized below in table 1; the time constant τ (J_m/B_m) was equal to 7.57 s.

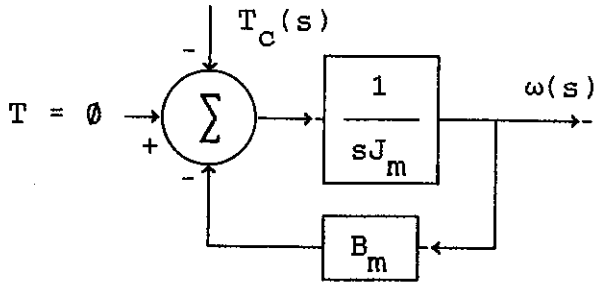

Figure 6. Block Diagram Representing Unloaded Motor with Armature Open Circuit

The Effect of the Viscous Friction Coefficient B_m

The expression ($B_mR_a + k_ek_T$) frequently appeared in the previous equations. From our model data, the term B_mR_a is approximately 1% of k_ek_T and thus may be neglected. Care must be taken, however, in neglecting the viscous friction term, as its value may rise rapidly with the application of any load to the motor. Also, B_m will be subsequently modified to include the effects of the generator and, more importantly, the load resistance. This modification results in an increased effective value of the total viscous friction of the system; under these conditions, this term in no longer negligible. For these reasons, the entire expression ($B_mR_a + k_ek_T$) will be retained in the model.

MODEL EXTENSION

Having already covered the development of the motor model in detail, the extension to the complete model shown in block diagram form in figure 7 is straightforward and is described in the following sections.

Table 1. Results of "Run Down" Tests on Motor

Initial speed $\omega(0)$, rpm	$(time)_{actual}$ to 36.8% of $\omega(0)$, s	$(time)_{predicted}$* to 36.8% of $\omega(0)$, s
2000	2.5	2.45
1500	2.3	2.00
1000	1.7	1.48

*based on equation (15)

Inclusion of the DC Generator and a Resistive Load

Methods for determining the moment of inertia J_g and the resistance R_g of the generator armature and the generator constant, k_g, are identical to those used for calculating the analogous values for the motor; again, the time constant, L_g/R_g, (for the generator) may be neglected. To determine the viscous friction coefficient B_g (of the generator), the method utilized to obtain the corresponding value for the motor is used. However, because the motor and generator are coupled, the slope of the resulting I_a versus ω graph (figure 4) is now equal to ($B_m + B_g$).

The measured values of the above parameters for the generator were of the same order of magnitude as those for the motor; this can be expected given the devices' similar physical size. The generator load, R_{load}, is included in the model as an equivalent friction term.

Because the power dissipated in the generator armature circuit is

$$P = \frac{\left(k_g\omega\right)^2}{R_g + R_{load}} \qquad (16)$$

and power dissipation due to viscous friction, B, at speed, ω, is $B\omega^2$ (remember: B = friction force PER UNIT SPEED), the electrical load may be represented as

$$\text{equivalent viscous friction coefficient due to generator load} = \frac{k_g^2}{R_g + R_{load}} \qquad (17)$$

To verify this value, the total effective viscous friction coefficient, B_T, which is defined below, was measured. With the motor driving the generator, which was connected to an 86 Ω load, a graph of I_a versus ω (figure 4) was again obtained, and the slope was measured to determine B_T. The value of [$B_T - (B_m + B_g)$] thus obtained compared well to the one calculated using equation (17), as they differed by

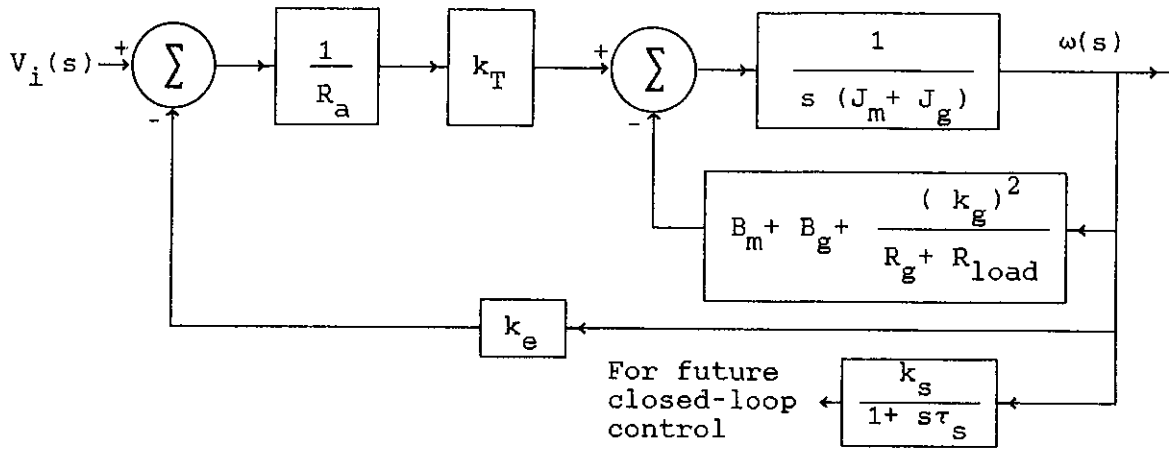

Figure 7. Complete Block Diagram for the Motor Driving the Generator Plus Load

only 5%. Hence, for the overall model, which includes a motor, a generator, and a load,

$$J_T = J_m + J_g \tag{18}$$

$$B_T = B_m + B_g + \frac{k_g^2}{R_g + R_{load}} \tag{19}$$

Block diagram reduction applied to figure 7 results in the transfer function

$$\frac{\omega(s)}{V_i(s)} = \frac{\dfrac{k_T}{B_T R_a + k_e k_t}}{1 + \dfrac{sJ_T R_a}{B_T R_a + k_e k_T}} \tag{20}$$

in which B_T and J_T are defined by equations (18) and (19).

Model Parameters for the DC Generator

Shown below are the values of the parameters for the Hampden type DCG-100 1/3 hp generator with a field voltage of 115 V.

$$J_g = 18.0 \times 10^{-4}\ \text{kg}\cdot\text{m}^2$$

$$B_g = 1.7 \times 10^{-4}\ \text{N}\cdot\text{m/rad/s}$$

$$k_g = 0.7\ \text{V/rad/s}$$

$$R_g = 15\ \Omega\ (\text{cold})$$

$$R_{load} = 86\ \Omega\ (110\ \text{W dissipation})$$

$$k_g^2/(R_g + R_{load}) = 48.5 \times 10^{-4}\ \text{N}\cdot\text{m/rad/s}$$

Speed Sensor Model

The dynamics of the speed sensor must be considered when measuring the open-loop and closed-loop responses of the system. The incremental encoder and its associated frequency-to-voltage unit may be represented initially as a block with first-order dynamics, that is

$$V_o(s)/\omega(s) = k_s/(1 + st_s)$$

The frequency-to-voltage converter is calibrated to have a gain of 10 V/20,000 Hz, while the encoder produces 500 pulses/rev. Hence,

$$k_s = \frac{500}{2\pi} \times \frac{10}{20{,}000}$$

$$= 4 \times 10^{-2}\ \text{V/rad/s}$$

A step-response test—from zero to full scale—in which a frequency-to-voltage converter was fed by a square wave generator while the output DC voltage was monitored on a storage oscilloscope revealed a time constant of $\tau_s = 15$ ms.

COMPARISON OF MEASURED AND MODEL-PREDICTED DYNAMIC RESPONSES

The simplified linear models previously developed for the unloaded motor; the motor and a generator; and a motor, a generator, and a load are all of the first order—see equations (12) and (20). Various tests involving step changes in V_i were conducted, and typical results are shown in figure 8. The speed changes were measured using the optical encoder and the frequency-to-voltage converter, and the output was displayed on a storage oscilloscope. Figure 8 also shows the predicted step response obtained using The Control System Design Program.[4] Conditions and equations for the simulation are given below. The time constant of the speed sensor is included in the simulation, as $\tau_s = 15$ ms is significant. The test results of figure 8 are for the motor, generator, and load, with

$$V_i = 101\ \text{V} \qquad R_{load} = 86\ \Omega \qquad \omega(0) = 0\ \text{rpm}$$

From equation (20), using the motor and generator parameters listed above, we obtain

$$\omega(s) = 1698/\left[1 + s\left(106.7 \times 10^{-3}\right)\right]\ \text{rpm for } V_i = 101\ \text{V}$$

Extending this to include the speed sensor response, we obtain

$$\omega(s) = \left[\frac{1698}{1 + s\left(106.7 \times 10^{-3}\right)}\right]\left[\frac{1}{1 + s\left(15 \times 10^{-3}\right)}\right]\ \text{rpm}$$

This must be rearranged into suitable form for entry into the program. Thus,

$$\omega(s) = \left(10.6 \times 10^5\right)/\left(s^2 + 76s + 625\right)\ \text{rpm}$$

It was found that the predicted and measured values of steady-state speed (1697 rpm and 1722 rpm, respectively) differ by approximately 1%, a value which we found typical for all tests. The predicted and measured time constants were 123 ms and 135 ms, respectively, an error of 9%. Generally, the values of the predicted and measured time constants differed by less than 10%. Note that these results will vary depending upon the temperature of both the field and the armature windings of the motor and generator. Increased temperatures will increase the resistance of each winding. Thus, the field current will decline and alter the motor

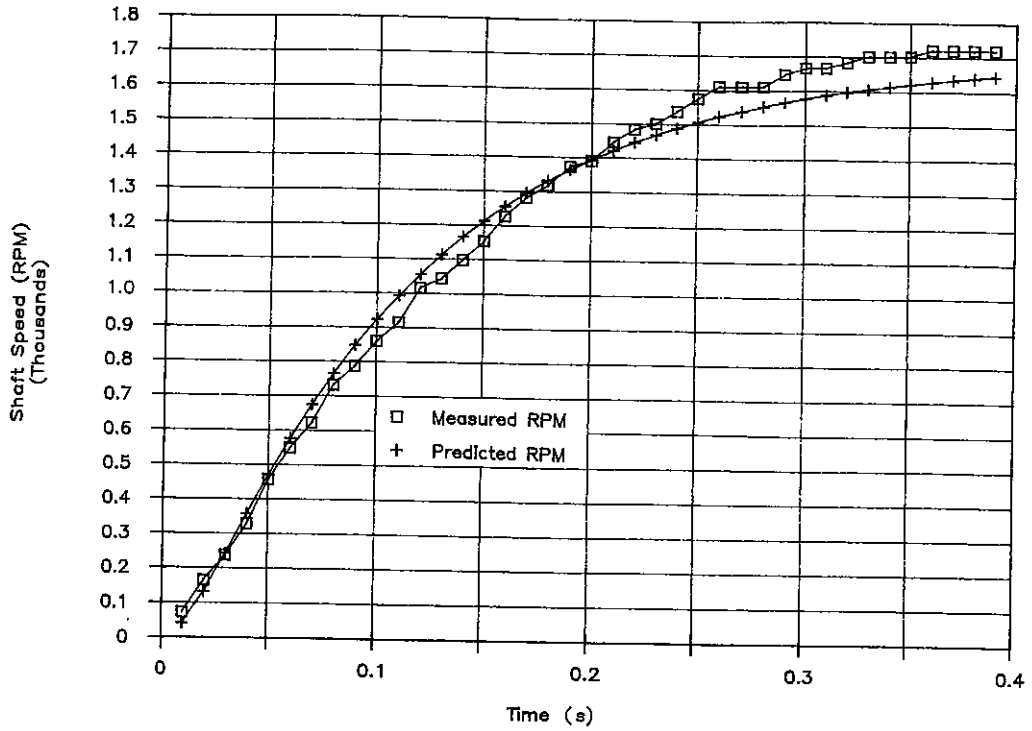

Figure 8. Comparison of Measured and Predicted Step Responses for the Motor, Generator, and 85 Ω Load

constants k_T and k_e. Increases in the armature resistance will tend to increase the time constant. Measurements and tests should, therefore, be conducted with the machines at stabilized running temperatures.

CONCLUSION

Details of the procedures used in the development of a simplified linear model to predict the dynamic behavior of a resistively loaded motor-generator set have been described. Comparison of the measured and predicted values reveals an error of less than 1% for steady-state speeds and a difference of less than 10% for the time constants.

Evaluation of the coefficients of the model by students may be achieved efficiently if the task is divided among groups working with similar equipment. Hence, J_m and R_a may be determined by one group; another could obtain the values of k_e and k_T; a third might calculate B_m and k_g, etc. Results may then be pooled, and the dynamic behavior of the group model can then be compared to that of the equipment associated with individual groups. The work is beneficial to students because it integrates topics such as Laplace transforms and differential equations, electrical machines, computing, rotational dynamics, and linear control theory—albeit at an introductory level.

For those readers interested in the model discussed above, a more detailed version of this paper is available from the lead author.

REFERENCES

1. McLean, D., "Mathematical Models of Electrical Machines," *Measurement and Control*, vol. 11, June 1978, pp. 231-36.
2. Sinha, N. K., C. D. diCenzo, and B. Szabados, "Modelling of DC Motors for Control Applications," *IEEE Trans. on Ind. Electronic & Control Inst.*, vol. IECI 21, no. 2, May 1974, pp. 84-88.
3. Program CC Version 3 DP, Release 3.51A, Hawthorne, Calif., Systems Technology, Inc.
4. Dorf, R. C., R. G. Jacquot, and S. D. Kirkish, *The Control System Design Program*, Addison-Wesley, Reading, Mass., 1988.
5. Richardson, D. V. and A. J. Caisse, Jr., *Rotating Electric Machinery and Transformer Technology*, Reston, Englewood Cliffs, N.J., 1987, pp. 130-35.
6. Aha, E., "DC Motors and Generators—A Tutorial Study," *Motion*, Jan./Feb. 1987, p. 7.
7. Gayakwad, R. and L. Sokoloff, *Analog and Digital Control Systems*, Prentice-Hall, Englewood Cliffs, N.J., 1988, pp. 123-24.
8. Szabados, B., C. D. diCenzo, and N. K. Sinha, "Dynamic Measurements of the Main Electrical Parameters of DC Machine," *IEEE Trans. on Industry and General Applications*, vol. 1GA-7, no. 1, Jan./Feb. 1971, pp. 109-14.
9. Meshkat, S., "Digital Signal Processors Provide Advanced Motion Control," *Power Conversion & Intelligent Motion*, Nov. 1987, pp. 55-61.

Anthony J. A. Oxtoby joined the EET Department of Purdue University as a visiting professor in January 1989. He was educated in England, where he obtained his BSc. Hons. degree in electronic engineering from the University of Hull in 1973 and his MSc. in systems and control from the University of Manchester in 1980. He has consulted in the area of industrial control systems and instrumentation.

Thomas L. Robertson is an associate professor in the EET Department at the Purdue University-West Lafayette campus. He holds a B.S. EET and an M.S. I.S. from Purdue and a Ph.D. in technical education from the University of Illinois. For the past ten years he has taught and consulted in the area of industrial controls and computers.

J. Michael Jacob is a professor in the EET Department of Purdue University. He received a B.S. in physics from North Carolina State University in 1969 and an M.S. in electrical engineering from the University of South Carolina in 1977. For the past ten years he has taught and consulted in advanced analog integrated circuits and process control. He is the author of two textbooks on industrial controls and analog electronics.